Saudi Pharmaceutical Journal 26 (2018) 801–809

Contents lists available at ScienceDirect

Saudi Pharmaceutical Journal

journal homepage: www.sciencedirect.com

Original article

New derivatives of hydrogenated pyrido[4,3-b]indoles as potential neuroprotectors: Synthesis, biological testing and solubility in pharmaceutically relevant solvents

Svetlana Blokhina [a], Angelica Sharapova [a,*], Marina Ol'khovich [a], Anatoly Ustinov [b], German Perlovich [a]

[a] Institute of Solution Chemistry, Russian Academy of Sciences, 1 Akademicheskaya Street, 153045 Ivanovo, Russia
[b] Institute of Physiologically Active Compounds, Russian Academy of Sciences, 142432 Chernogolovka, Russia

ARTICLE INFO

Article history:
Received 12 December 2017
Accepted 2 April 2018
Available online 6 April 2018

Keywords:
Novel bioactive compounds
Neurocorrection activity
Thermophysical properties
Dissolution

ABSTRACT

The derivatives of hydrogenated pyrido[4,3-b]indoles as potential neuroprotectors have been synthesized. The different substituents were introduced into position 8 of the carboline fragment of the molecule: methyl-, methoxy-, fluorine- and chlorine-. Biological tests have shown that all the studied compounds can modulate glutamate-dependent uptake of calcium ions in rats' cerebral cortex synaptosomes. The shake-flask method was used to measure the solubility of the compounds in the buffer solution (pH 7.4), hexane and 1-octanol within the temperature interval of 293.15–313.15 K. All the derivatives have been found to have low solubility (not exceeding $8 \cdot 10^{-4}$ mole fractions) in the mentioned solvents. The effect of thermophysical and protolytic properties of the compounds on the solubility have been studied and the thermodynamic functions of compounds dissolution in the solvents used have been calculated.

1. Introduction

A number of the most important drug structures have been identified by analyzing the results of experimental bioscreening of a large set of substances, their medical applications and structural data (Rekker and Mannhold, 1992). Among them are pyrido[4,3-b]indole derivatives with a wide range of biological activity: antihistamine, central depressant, anti-inflammatory, neuroleptic and other types (Ivachtchenko et al., 2010; Stefek et al., 2011; Dondas et al., 2016). The structural analogues of this series, and the antihistamine drug Dimebon (Latrepirdine) in particular, were found to slow down the neurodegenerative process (Ikonomidou and Turski, 2002; Doody et al., 2008). Although Dimebon had not passed the final clinical tests, it stimulated new research aimed at studying molecular mechanisms of its activity and developing its efficient structural analogues (Eckert et al., 2012; Steele and Gandy, 2013; Hung et al., 2015). The aim of this work is to synthesize new Dimebon derivatives too.

According to the modern understanding of the Alzheimer's disease pathogenesis, the key factor in the development of neurodegenerative processes in human brain is the pathological form of amyloid peptide. Neurodegenerative processes caused by β-peptide include calcium homeostasis disorder, higher levels of oxidative stress, potentiation of toxicity of excitatory neurotransmitter amino acids, and cell death initiation (Mattson et al., 1992). Abnormal increase in calcium ion concentration in body cells is known to trigger a series of degenerative processes accompanying body aging. Calcium homeostasis disorder is the basis of the calcium theory of aging and dementia (Khachaturian, 1994). Scientists are now working on a whole range of approaches to prevention and correction of cell neurodegeneration including development of blocking agents of glutamate-induced calcium ion influx as potential neuroprotectors with a high biological activity (Parsons et al., 1998; Farlow, 2004).

Drug delivery plays an important role in creating biologically active compounds, along with specific interactions with ferments and receptors. A medicinal drug is expected to have a number of physical and chemical properties ensuring its distribution in the body. Among the most important properties is drug solubility in pharmaceutically relevant media that influences the drug ability

* Corresponding author.
E-mail address: avs@isc-ras.ru (A. Sharapova).

Peer review under responsibility of King Saud University.

Production and hosting by Elsevier

https://doi.org/10.1016/j.jsps.2018.04.003
1319-0164/

to overcome biological barriers, including the blood-brain barrier. Physicochemical properties of medicinal drugs, their structure and experimental data about solubility are now widely used to develop new methods of predicting solubility of biologically active compounds (Avdeef, 2007; Faller and Erlt, 2007). But, despite a considerable progress in modeling methods, the accuracy of calculating the solubility of compounds with a big molecular weight and containing several functional groups remains rather low (Du-Cuny et al., 2008).

Among such complex molecular structures are representatives of the γ-carboline series – derivatives of hydrogenated pyrido [4,3-b]indoles. Synthesis of new substances and revealing the dependence of their biological activity on physicochemical properties and molecular structure is the basis of the research direction named QSAR (Quantitative Structure-Activity Relationship) in modern medicinal chemistry (Danishuddin and Khan, 2016). To date it is largely unknown how different functional groups introduced into a molecule change the substance influence on the body (Waterbeemd and Rose, 2008; Asirvatham et al., 2016). Solving this problem could help optimize the molecular design aimed at developing efficient drugs with predictable biological activity. The aim of the work was to synthesize heterocyclic derivatives of tetrahy dro-1H-pyrido[4,3-b]indole with substituents of different chemical nature in the carboline fragment, to study their neurocorrection activity, thermophysical properties and solubility in pharmaceutically relevant media. This work is a continuation of our studies of biological activity, solubility, lipophilicity and membrane permeability of drugs and drug-like compounds (Perlovich et al., 2006; Blokhina et al., 2014; Sharapova et al., 2017).

2. Experimental section

2.1. General

All the chemicals were of reagent grade, purchased from commercial sources and used without further purification. Dimebon with 98% purity was purchased from Sigma-Aldrich (Saint Louis, MO, USA). The solvents used, namely 1-octanol and hexane from Merck, were of the highest purity. ^{1}H and ^{13}C NMR spectra were recorded on a Bruker CXP-200 (Germany) (200.13 and 50.04 MHz, respectively). The chemical shift values are given in the δ scale relative to Me_4Si. Mass spectra were recorded on a Finnigan 4021 mass spectrometer operating at 70 eV. Elemental analyses were determined on a Carlo-Erba CHN analyzer.

2.2. Synthesis and characterization of compounds

The synthetic goal of the work was to obtain new compounds of the carboline series – "direct analogues" of Dimebon possessing neurocorrecting activity. Dimebon modification consists in introducing a triazole cycle instead of the pyridyl one. The target compounds G4 were prepared using the synthetic route shown in Scheme 1. The pyrido[4,3-b]indoles (**G1**) were prepared by the Fischer reaction. Pyrido [4,3-b] indoles G1 were attached to ethyl acrylate in the presence of Triton B in boiling benzene to give esters G2. The latter were converted by hydrazine hydrate to the corresponding hydrazides G3. The reaction of hydrazides of carboxylic acids and methyl isothiocyanate in boiling ethanol leads to 2,4-dihydro-1,2,4-triazole-3-thiones G4. The structures of these synthesized compounds were characterized by ^{1}H NMR, ^{13}C NMR, MS methods and elemental analysis. In the ^{1}H NMR spectra in the 9–11 ppm range there are no signals of NH-group protons of intermediate thiosemicarbazides, but a signal is observed in the range 13.37–13.54 ppm characteristic for 1,2,4-triazoles. Absence of a signal of the proton of the SH group in NMR spectra indicated that synthesized 1,2,4-triazoles are present in thione form.

2.2.1. Synthesis of 3-(2-Methyl-2,3,4,5-tetrahydropyrido[4,3-b]indol-5-yl)propionic acid ethyl ester (*G2*)

A solution of benzyltrimethylammonium hydroxide (40 wt.% in methanol, 3.5 ml) was added to a solution of **G1** (17.114 g, 92 mmol) containing a mixture of benzene (170 ml) and ethyl acrylate (75 ml). The mixture was heated under reflux for 7 h, cooled, washed with water, and extracted with 2 M HCl. The acidic solution was extracted with benzene, basified with 10% NaOH, and extracted with benzene. The combined extracts were washed with water, dried and evaporated to an oil (21.18 g, 80%).

2.2.2. Synthesis of 3-(2-Methyl-2,3,4,5-tetrahydropyrido[4,3-b]indol-5-yl)propionic acid hydrazide (*G3*)

Hydrazine monohydrate (20 mL, 0.41 mol) was added to a solution of **G2** (20.356 g, 0.071 mol) in ethanol (50 mL), and the mixture was heated under reflux for 2 h 30 min. After 72-h storage at −12 °C, the resulting crystals were collected, washed with 2-propanol, and dried to produce 12.7 g (65.6%) of **G3**, mp 123–124 °C. ^{1}H NMR (DMSO-d_6/$CDCl_3$, 1:1, δ, ppm, J/Hz): 9.07 (s, 1H, NH), 7.32 (m, 2H, H_{arom}), 7.01 (m, 2H, H_{arom}), 4.30 (t, 2H, J = 6.7), 4.05 (br s, 2H, NH_2), 3.54 (s, 2H, $MeNCH_2$), 2,75 (m, 4H, $MeNCH_2$-CH_2), 2.47 (m, 5H, CH_2, Me).

Other acid hydrazides **G3** were prepared by the above-mentioned method for compound **I**.

3-(2,8-Dimethyl-1,2,3,4-tetrahydropyrido[4,3-b]indol-5-yl)propio nic acid hydrazide was prepared in 73% yield, mp 163.5–165.5 °C. ^{1}H NMR ($CDCl_3$, δ, ppm, J/Hz): 7.14 (m, 2H, H_{arom}), 7.02 (br, s, NH), 6.95 (dd,1H, H_{arom}, J = 8.6, J = 1.2), 4.31 (t, 2H, CH_2, J = 6.6), 3.59 (s, 2H, $MeNCH_2$), 3.48 (br s, 2H, NH_2), 2.78 (s, 4H,$MeNCH_2$-CH_2), 2.51 (s, 3H, Me), 2.42 (m, 5H, CH_2, Me).

3-(8-Methoxy-2-methyl-1,2,3,4-tetrahydropyrido[4,3-b]indol-5-y l) propionic acid hydrazide was prepared in 44.6% yield, mp 126.5–127.5 °C. ^{1}H NMR (DMSO-d_6/$CDCl_3$, 1:1, δ, ppm, J/Hz): 9.05 (s, 1H, NH), 7.23 (d, H_{arom}, J = 8.6), 6.79 (d, 1H, H_{arom}, J = 2.2), 6.69 (dd, 1H, H_{arom}, J = 8.6, J = 2.2), 4.25 (t, 2H, CH_2, J = 7.0), 3.76 (s, 3H, MeO), 3.51 (s, 2H, $MeNCH_2$), 2.79 (m, 4H, $MeNCH_2CH_2$), 2.42 (m, 5H, CH_2, Me).

3-(8-Fluoro-2-methyl-1,2,3,4-tetrahydropyrido[4,3-b]indol-5-yl) propionic acid hydrazide was prepared in 72% yield, mp 158–159 °C. ^{1}H NMR (DMSO-d_6/$CDCl_3$, 1:1, δ, ppm, J/Hz): 9.06 (s, 1H, NH), 7.35 (dd, 1H, H_{arom}, J = 8.6, J = 4.5), 7.00 (dd, 1H, H_{arom}, J = 9.6, J = 2.5), 6.84 (td, 1H, H_{arom}, J = 9.2, J = 2.5), 4.29 (t, 2H, J = 6.7), 4.06 (br s, 2H, NH_2), 3.49 (s, 2H, $MeNCH_2$), 2.79 (m, 4H, $MeNCH_2CH_2$), 2.46 (m, 5H, CH_2, Me).

3-(8-Chloro-2-methyl-1,2,3,4-tetrahydropyrido[4,3-b]indol-5-yl) propionic acid hydrazide was prepared in 74% yield, mp 172–173 °C. ^{1}H NMR (DMSO-d_6/$CDCl_3$, 1:1, δ, ppm, J/Hz): 9.06 (s,1H, NH), 7.35 (d, 1H, H_{arom}, J = 8.6), 7.29 (d, 1H, H_{arom}, J = 1.9), 7.02 (dd, 1H, H_{arom}, J = 8.6, J = 1.9), 4.29 (t, 2H, CH_2, J = 6.7), 4.01 (br S, 2H, NH_2), 3.50 (s, 2H, $MeCH_2$), 2.80 (m, 4H, $MeNCH_2CH_2$), 2.46 (m, 5H, CH_2, Me).

2.2.3. Synthesis of 4-Methyl-5-[2-(2-methyl-1,2,3,4-tetrahydropyrido [4,3-b]indol-5-yl)ethyl]-2,4-dihydro[1,2,4]triazole-3-thione (*G4 - compound I*)

A mixture of 2.187 g (8 mmol) 3-(2-methyl-1,2,3,4-tetrahydro pyrido[4,3-b]indol-5-yl)-propionic acid hydrazide, 0.587 g (8 mmol) methyl isothiocyanate and 55 ml of ethanol was heated under reflux for 6 h 30 min and then left for 48 h at ambient temperature. The resulting crystals were collected, washed with ethanol, and dried. Yield 2.268 g (86%), mp 216–219 °C (EtOH). Found: C 62.58; H 6.54; N 21.27%. Calcd for $C_{17}H_{21}N_5S$: C 62.36; H 6.46; N 21.39; S 9.79%. ^{1}H NMR (DMSO-d_6/$CDCl_3$, 1:1, δ, ppm, J/Hz): 13.51 (br s, 1H in exchange, NH), 7.31 (m, 2H, H_{arom}), 7.04 (m, 2H, H_{arom}),

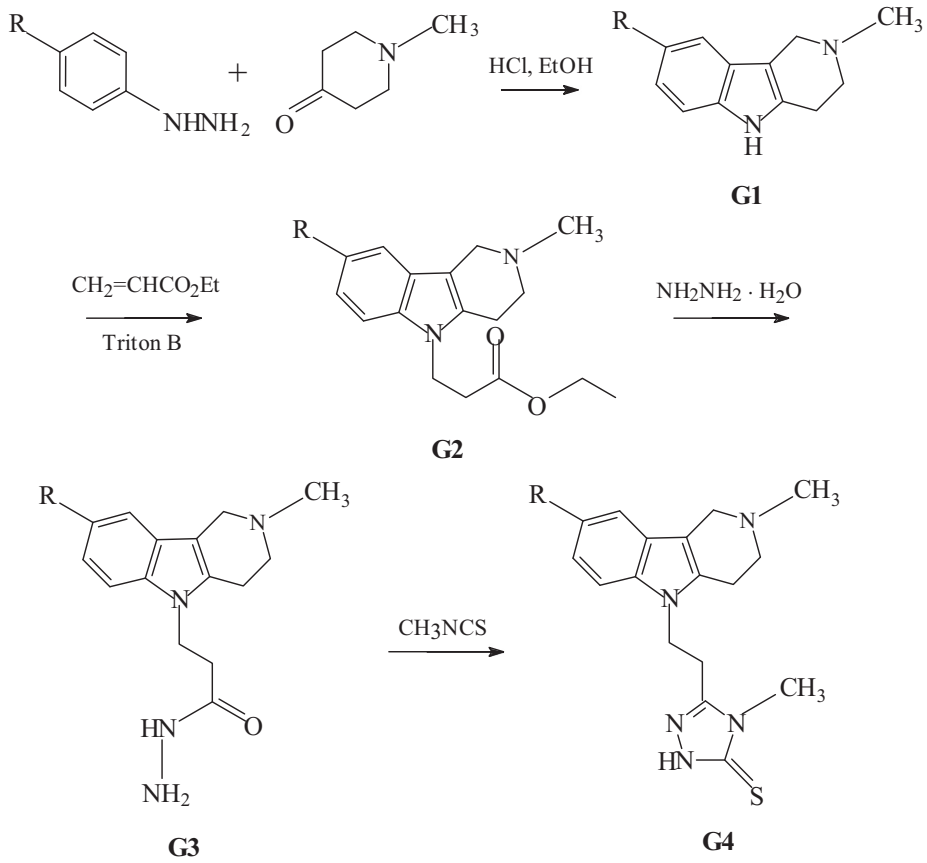

Scheme 1. Synthesis of 2,4-dihydro-1,2,4-triazole-3-thiones: R – H (I); –CH_3 (II); -OCH_3 (III); -F (IV); -Cl (V).

4.43 (t, 2H, CH_2, J = 6.9), 3.56 (s, 2H, $MeNCH_2$), 3.15 (s, 3H, Me), 3.06 (t, 2H, CH_2, J = 6.9), 2.75 (s, 4H, $MeNCH_2CH_2$), 2.48 (s, 3H, Me). ^{13}C NMR (DMSO-d_6, δ, ppm): 166.55, 150.21, 135.52, 133.26, 125.14, 120.40, 118.67, 117.22, 108.94, 107.54, 51.88, 51.15, 45.32, 29.32, 25.68, 21.82. MS (m/z): 327 (M^+).

Other 2,4-dihydro-1,2,4-triazole-3-thiones were prepared by the above-mentioned method for compound **I**.

5-[2-(2,8-Dimethyl-1,2,3,4-tetrahydropyrido[4,3-b]indol-5-yl)ethyl]-4-methyl-2,4-dihydro [1,2,4] triazole-3-thione (compound **II**). Yield 80%, mp 219–222 °C (EtOH). Found: C 63.52; H 6.73; N20.64%. Calcd for $C_{18}H_{23}N_5S$: C 63.31; H 6.79; N 20.51; S 9.39%. ^{1}H NMR (DMSO-d_6/$CDCl_3$, 1:1, δ, ppm, J/Hz): 13.37(br s, 1H in exchange, NH), 7.14 (m, 2H, H_{arom}), 6.90 (dd, 1H, H_{arom}, J = 8.3, J = 1.3), 4.39 (t, 2H, CH_2, J = 6.9), 3.54 (s, 2H, $MeNCH_2$), 3.13 (s, 3H, Me), 3.03 (t, 2H, CH_2, J = 6.9), 2.73 (m, 4H, $MeNCH_2CH_2$), 2.48 (s, 3H, Me), 2.39 (s, 3H, Me). ^{13}C NMR (DMSO-d_6, δ, ppm): 166.53, 150.25, 133.97, 133.26, 127.12, 125.36, 121.85, 117.03, 108.65, 107.04, 51.89, 51.18, 45.32, 29.32, 25.70, 21.83, 21.05. MS (m/z): 341 (M^+).

5-[2-(8-Methoxy-2-methyl-1,2,3,4-tetrahydropyrido[4,3-b]indol-5-yl)ethyl]-4-methyl-2,4-dihydro[1,2,4]triazole-3-thione (compound **III**). Yield 93%, mp 219–222 °C (EtOH). Found: C 60.71; H 6.54; N 19.47%. Calcd for $C_{18}H_{23}N_5OS$: C 60.48; H 6.49; N 19.59; O 4.48; S 8.97%. ^{1}H NMR (DMSO-d_6/$CDCl_3$, 1:1, δ, ppm, J/Hz): 13.51 (br s, 1H in exchange, NH), 7.18 (d, 1H, H_{arom}, J = 8.8), 6.82 (d, 1H, H_{arom}, J = 1.9), 6.70 (dd, 1H, H_{arom}, J = 8.8, J = 1,9), 4.39 (t, 2H, CH_2, J = 6.7), 3.78 (s, 3H, MeO), 3.53 (s, 2H, $MeNCH_2$), 3.13 (s, 3H, Me), 3.03 (t, 2H, CH_2, J = 6.8), 2.72 (m, 4H, $MeNCH_2CH_2$), 2.47 (s, 3H, Me). ^{13}C NMR (DMSO-d_6, δ, ppm): 166.51, 153.20, 150.27, 133.83, 130.66, 125.48, 109.78, 109.58, 107.28, 99.76, 55.21, 51.89, 51.26, 45.32, 29.30 25.75, 21.90. MS (m/z): 357 (M^+).

5-[2-(8-Fluoro-2-methyl-1,2,3,4-tetrahydropyrido[4,3-b]indol-5-yl)ethyl]-4-methyl-2,4-dihydro[1,2,4]triazole-3-thione (compound **IV**). Yield 83%, mp 215–218 °C (EtOH). Found: C 59.39; H 5.75; N 20.38%. Calcd for $C_{17}H_{20}FN_5S$: C 59.11; H 5.84; F 5.50; N 20.27; S 9.28%. ^{1}H NMR (DMSO-d_6/$CDCl_3$, 1:1, δ, ppm, J/Hz): 13.49 (br s, 1H in exchange, NH), 7.26 (dd, 1H, H_{arom}, J = 8.9, J = 4.4), 7.03 (dd, 1H, H_{arom}, J = 9.6, J = 2.4), 6.84 (td, 1H, H_{arom}, J = 9.2, J = 2.4), 4.43 (t, 2H, CH_2, J = 7.0), 3.52 (s, 2H, $MeNCH_2$), 3.16 (s, 3H, Me), 3.05 (t, 2H, CH_2, J = 7.0), 2.75 (s, 4H, $MeNCH_2CH_2$), 2.48 (s, 3H, Me). ^{13}C NMR (DMSO-d_6, δ, ppm, J/Hz): 166.57, 156.82 (d, $^1J_{CF}$ = 231.4), 150.16, 135.47, 132.22, 125.32 (d, $^3J_{CF}$ = 9.9), 109.91 (d, $^3J_{CF}$ = 9.6), 108.06 (d, $^2J_{CF}$ = 22.1), 107.75, 102.33 (d, $^2J_{CF}$ = 23.2), 51.76, 50.99, 45.27, 29.34, 25.67, 21.95. MS (m/z): 345 (M^+).

5-[2-(8-Chloro-2-methyl-1,2,3,4-tetrahydropyrido[4,3-b]indol-5-yl)ethyl]-4-methyl-2,4-dihydro[1,2,4]triazole-3-thione (compound **V**). Yield 88%, mp 216–219 °C (EtOH). Found: C 56.17; H 5.64; N 19.47%. Calcd for $C_{17}H_{20}ClN_5S$: C 56.42; H 5.57; Cl 9.80; N 19.35; S 8.86%. ^{1}H NMR (DMSO-d_6/$CDCl_3$, 1:1, δ, ppm, J/Hz): 13.54 (br s, 1H in exchange, NH), 7.32 (d, 1H, H_{arom}, J = 1.9), 7.27 (d, 1H, H_{arom}, J = 8.7), 7.02 (dd, 1H, H_{arom}, J = 8.7, J = 1.9), 4.43 (t, 2H, CH_2, J = 6.8), 3.53 (s, 2H, $MeNCH_2$), 3.18 (s, 3H, Me), 3.05 (t, 2H, CH_2, J = 6.8), 2.75 (s, 4H, $MeNCH_2CH_2$), 2.48 (s, 3H, Me). ^{13}C NMR (DMSO-d_6, δ, ppm): 166.56, 150.09, 135.32, 134.06, 126.19, 123.38, 120.10, 116.60, 110.54, 107.50, 51.70, 50.83, 45.24, 29.37, 25.62, 21.86. MS (m/z): 361 (M^+).

2.3. Biological activity

Determination of the effect of compounds on glutamate-induced $^{45}Ca^{2+}$ uptake into synaptosomes of rat brain cortex was performed according to the method presented in the work (Hung

et al., 2015). The interaction between the compounds and the glutamate-dependent calcium uptake system was studied on P_2-fraction of mitochondrial crude synaptosomes (Gylys et al., 2000). obtained from celebral cortex of newborn (9–10 days) Wistar rats using the standard Hajos method (Hajos, 1975). The brain was homogenized with 10 volumes of cooled 0.32 M sucrose at 900 rpm. The homogenate was centrifuged at 1500 g for 10 min, and the resulting supernatant was centrifuged at 10,000 g for 20 min. The radioactive label was accumulated by suspension of the synaptosomals P_2-fraction in the incubation buffer A having the following composition: 132 mM NaCl, 5 mM KCl, 5 mM HEPES, 10 mM glucose, pH 7.4 (protein concentration of approximately 1.5–2 mg/ml). The biological activity of the synthesized derivatives was studied by adding 50 μl of buffer A to the incubation medium with the substance studied in the concentration range of 0.01–100 μM. The mixture was further incubated for 5 min with 200 μM of glutamate at 37 °C and then the $^{45}Ca^{2+}$ uptake was stopped by filtration through GF/B-filters (Whatman, England) followed by three washes with cold buffer B (145 mM KCl, 10 mM Tris, 5 mM Trilon B, pH 7.4). The radioactivity probes were analyzed by a fluid scintillation β-analyzer (TriCarb, Perkin Elmer). All the tests were performed in three parallel trials in 2–3 independent experiments. The $^{45}Ca^{2+}$ uptake amount was estimated by calculating the difference of radioactive label during stimulation with glutamate and without stimulation with an agonist. The result is presented as percents with respect to the control measurement which was 100%. NMDA-antagonist Dizocilpine (MK-801) has been used for positive Control. MK-801 with purity 98% was purchased from Sigma-Aldrich (Saint Louis, MO, USA). The specific $^{45}Ca^{2+}$uptake was estimated using the following equation:

$$\text{Percentage } {}^{45}Ca^{2+} \text{ of Control} = [(Ca_4 - Ca_3)/(Ca_2 - Ca_1)] \cdot 100\% \quad (1)$$

where Ca_1 - $^{45}Ca^{2+}$ is the uptake for the Control (without glutamate and the tested compound), Ca_2 is the glutamate-induced $^{45}Ca^{2+}$ uptake (glutamate only), Ca_3 - $^{45}Ca^{2+}$ is the uptake in the presence of the tested compound (without glutamate), Ca_4 - $^{45}Ca^{2+}$ is the uptake in the presence of glutamate and the tested compound.

2.4. Differential scanning calorimetry

Fusion temperatures and enthalpies of the compounds under investigation have been determined using a Perkin-Elmer Pyris 1 DSC differential scanning calorimeter (Perkin-Elmer Analytical Instruments, Norwalk, Connecticut, USA) with Pyris software for Windows NT. DSC runs were performed in an atmosphere of flowing 20 cm^3/min dry helium gas of high purity 0.99996 (mass fraction) using standard aluminum sample pans and a heating rate of 2 °C/min. The accuracy of weight measurements was 0.005 mg. The DSC was calibrated using two-point calibration, measuring the onset temperatures of indium and zinc standards. The onset of melting was used for calibration because it is almost independent of the scan rate. The melting temperatures for indium and zinc were 156.6 and 419.5 °C, respectively (determined by at least ten measurements). The enthalpy scale was calibrated using the indium fusion heat. The measured value of the fusion enthalpy corresponded to 28.69 J/g (the reference value was 28.66 J/g (Archer et al., 2003). The standard uncertainty of the melting temperature was determined as twice the standard deviation of five independent measurements.

2.5. Solubility

The saturated equilibrium solubility of the studied compound was determined by the shake flask method at atmospheric pressure and in the temperature range from 293.15 K to 313.15 K. The essence of the above mentioned method consists in determination of the compound concentration in the saturated solution. An excess amount of the compound was added to the known amount of various pure solvents in triplicate. The concentrated compound suspensions in each solvent were shaken continuously in an air thermostat containing a stirring device. The point of the solution thermodynamic equilibrium was determined based on the solubility kinetic dependences and averaged 72 h. The solid phase sedimentation time after stirring was 4 h. After the saturation was achieved, the solution aliquot was taken and centrifuged in a centrifuge Biofuge stratus (Germany) for 5 min at a fixed temperature. Then, the supernatant solutions were filtered through a 0.45 μm filter MILLEX®HA (Ireland). The saturated solution was diluted with the corresponding solvent to the required concentration. The concentration in molarity was assessed by measuring the absorbance at the wavelength of 329 nm using a UV–vis spectrophotometer (Cary-50, USA) at room temperature.

The calibration procedure was conducted at room temperature using the solutions with known concentrations of each substance in each investigated solvent. The solutions were prepared by adding an appropriate mass of the substance and volume of the solvent (1-octanol, hexane) to the flask and mixing until the substance was totally dissolved. The absorbance of the solutions was measured and the calibration curves were constructed. The calibration curve was observed to be linear in the concentration range of 0.2–1.0 μg ml^{-1} with a correlation coefficient of 0.9995. The experimental setup and its accuracy were validated by comparing the experimental solubility data of benzoic acid in water with those in (Stephen and Stephen, 1963). The deviation of the measured solubilities from the literature values did not exceed 1%.

The standard Gibbs energies of the dissolution processes ΔG^0_{sol} were calculated using the following equation:

$$\Delta G^0_{sol} = -RT \ln a_2 \quad (2)$$

where $a_2 = \gamma_2 x_2$ is the activity of the solute molecule; x is the drug molar fraction in the saturated solution; γ_2 is the activity coefficient of the solute molecule. The standard solution enthalpies ΔH^0_{sol} were calculated using the van't Hoff equation:

$$\partial(\ln a_2)/\partial T = \Delta H^0_{sol}/RT^2 \quad (3)$$

Due to very low solubilities of the compounds under investigation in buffer solutions it was assumed that $\gamma_2 = 1$. The temperature dependences of drug solubilities within the chosen temperature interval can be described by the linear function:

$$\ln x = A - B/T \quad (4)$$

This indicates that the change in heat capacity of the solutions with the temperature is negligibly small.

The standard solution entropies ΔS^0_{sol} were obtained from the well-known equation:

$$\Delta G^0_{sol} = \Delta H^0_{sol} - T\Delta S^0_{sol} \quad (5)$$

3. Results and discussion

3.1. Biological activity

In order to develop medicinal drugs with neurocorrecting activity, the derivatives of the hydrogenated pyrido[4,5-b]indoles (**I–V**) were synthesized, the structural formulae of which are given in Scheme 1. Since the target of Dimebon and, consequently, of the obtained compounds is the glutamatergic system of the central nervous system, the *in vitro* studies of their physiological activity

Table 1
Effect of compounds studied on glutamate-induced $^{45}Ca^{2+}$ uptake into synaptosomes of rat cortex.

Concentration, μM	Percentage $^{45}Ca^{2+}$ of Control (Control – 100%)						
	MK-801	I	II	III	IV	V	Dimebon
0.01	99.7	–	84.7 ± 1.2	86.7 ± 4.0	102.0 ± 9.8	103.5 ± 7.7	–
0.1	98.9	90.5 ± 5.1	85.5 ± 3.9	57.5 ± 8.3	78.7 ± 10.3	95.3 ± 1.0	120.5 ± 3.3
0.5	98.4	94.8 ± 3.0	102.6 ± 3.6	83.0 ± 7.9	78.7 ± 8.0	102.2 ± 6.3	64.4 ± 12.4
1	97.5	94.5 ± 11.8	93.6 ± 3.6	83.4 ± 12.7	83.2 ± 10.9	94.5 ± 4.7	61.3 ± 8.1
5	76.1	80.0 ± 3.0	113.1 ± 7.6	86.6 ± 4.5	94.7 ± 8.5	80.7 ± 10.5	83.2 ± 4.1
10	65.2	69.9 ± 4.4	109.7 ± 7.5	85.8 ± 15.2	93.4 ± 6.9	75.6 ± 10.0	89.3 ± 1.2
50	35.0	90.0 ± 6.1	118.6 ± 2.7	93.1 ± 12.8	96.9 ± 6.0	93.3 ± 11.0	98.7 ± 8.8
100	26.9	104.2 ± 12.8	127.1 ± 17.1	96.1 ± 13.2	87.1 ± 11.5	135.5 ± 9.4	132.0 ± 2.9

were conducted on the P_2-fraction of synaptosomes of rat celebral cortex containing NMDA, kainate and metabotropic receptors of type I. The synthesized compounds have been found to be able to modulate the glutamate-dependent uptake of calcium ions in rat cerebral cortex synaptosomes. The results of studying the biological activity of the synthesized compounds are given in Table 1 and Fig. 1. As these data show, the concentration dependences of the inhibitory factor have a dome shape, just like those of Dimebon.

Compound **I** did not affect glutamate-induced calcium ion uptake into synaptosomes of rat cortex at a concentration of 0.1–1.0 μM. At the concentrations of 5–50 μM, this compound inhibited calcium ion uptake. The maximum inhibition was 30% at the substance concentration of 30 μM. Compound **II** inhibited glutamate-induced uptake of calcium ions into the synaptosomes (inhibition ~ 15%) at the concentration of 0.01–0.1 μM. At the concentrations of 5–100 μM, the studied compounds caused an increased uptake of calcium ions into the synaptosomes (109–127% of control). The inhibiting ability of compound **III** becomes apparent at the concentration of 0.01–10 μM, with the maximal calcium ion uptake observed at the concentration of 0.1 μM (42.5%). Compound **IV** can act as an inhibitor in this test at the concentration of 0.1–1 μM and had no effect at the concentration of 5–100 μM. The inhibition of glutamate-induced calcium ion uptake with compound **V** is most efficient (~20%) at the concentration of 5–10 μM. The increase in the calcium ion uptake into the rat cortex synaptosomes is observed at the concentration of 100 μM (135.5%). As the obtained results show, all the studied compounds have inhibiting activity in this test. And their biological activity depends on the chemical nature of the substituent introduced into position 8 of the tetra-hydro-1H-pyrido[4,3-b]indole fragment of the molecule. The highest inhibiting activity within a wide concentration range (0.01–10 μM) comparable to the Dimebon action (Table 1) was found in compound **III** with a methoxy-substitutent, which allows to recommend it for further studies. Compounds **IV** and **V** with fluorine and chlorine atoms as substituents are weak inhibitors of calcium ion uptake, and methyl-derivative **II** even potentiates the uptake at high concentrations. Besides, by comparing the inhibiting ability of compound **II** and Dimebon (Fig. 1), can conclude that the biological activity of the studied compounds depends both on the substituent nature in the tetrahydro-carboline group and on the structure of the fragment bound through an ethyl linker connected to the nitrogen atom of the pyrrole cycle.

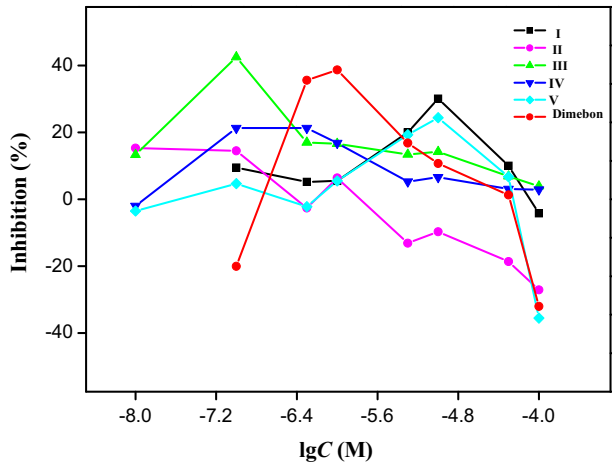

Fig. 1. Glutamate-induced $^{45}Ca^{2+}$ uptake into synaptosomes of rat cortex at different concentrations (lgC) of compounds studied introduced into the incubation mixture of the suspension of synaptosomes.

3.2. Thermophysical properties

The thermophysical properties of the synthesized compounds were studied by the DSC method. The results of these studies are given in Table 2. The DSC curves shown in Fig. 2 allow to conclude that the compounds do not have polymorphic modifications and are stable when heated to melting temperatures. The obtained melting temperature values are within the range of 234.1–276.0 °C, while the melting enthalpies vary in the range of 39.7–53.6 kJ/mol. Derivative **II** with a methyl substituent has the highest melting temperature and enthalpy. Replacing the fluorine atom with a chlorine one in the molecular structure of compound **IV** and the

Table 2
Physico-chemical characteristics of compounds studied.

Compound	[a]M (g/mol)	[b]T_m (°C)	[c]H_m (kJ/mol)	[d]pK_a
I	327.45	234.1 ± 0.2	44.3 ± 0.5	9.65 ± 0.2
II	341.46	276.0 ± 0.2	53.6 ± 0.5	9.63 ± 0.2
III	357.47	254.5 ± 0.2	39.7 ± 0.5	9.62 ± 0.2
IV	345.44	272.7 ± 0.2	41.1 ± 0.5	9.62 ± 0.2
V	361.89	245.9 ± 0.2	40.9 ± 0.5	9.61 ± 0.2

[a] M – molecular mass of compound.
[b] T_m – melting temperature of compound.
[c] H_m – melting enthalpy of compound.
[d] Calculated using Advanced Chemistry Development (ACD/Labs) Software V11.02.

transition to the structure of compound **V** result in a melting temperature increase but do not change the melting enthalpy.

3.3. Solubility in pharmaceutically relevant solvents

The classical saturation shake-flask method to measure the solubility of the synthesized substances have been used as it produces the most accurate results even for poorly soluble compounds (Baka et al., 2008). A buffer pH 7.4 simulating blood plasma and 1-octanol modeling membrane lipid layer were used as solvents (Kerns and Di, 2008). In order to find out the capacity of the studied organic substances for specific interactions, hexane was selected that interacts with the dissolved substance only through the van-der-Waals forces.

The solubility of the studied derivatives of hydrogenated pyrido [4,3-b]indoles (**I**–**V**) was measured in the buffer solution (pH 7.4), 1-octanol and hexane in the temperature range of 293.15–313.15 K (Table 3). Fig. 3 shows temperature dependences of compound **I** solubility as an example. Solubility of organic substances depends on whether the molecules are in the charged or neutral state in the water solution (Avdeef, 2007). The molecules of the studied compounds belong to the γ-carboline class, have a tetracyclic structure and contain an N-acceptor fragment (the main atom is N in the heterocycle) and an N-donor fragment (acidic secondary amino

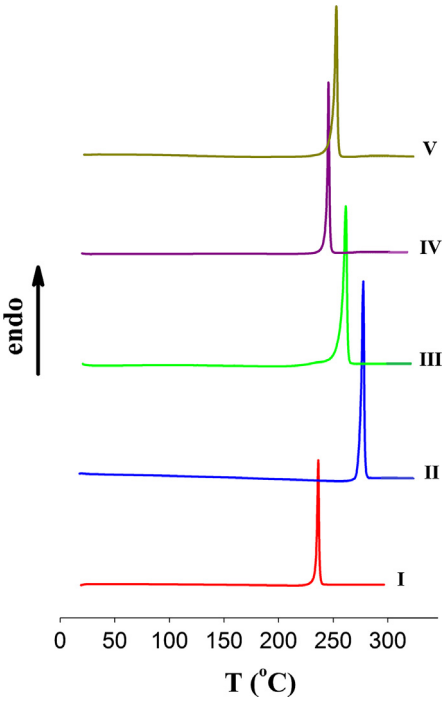

Fig. 2. DSC-curves of compounds studied.

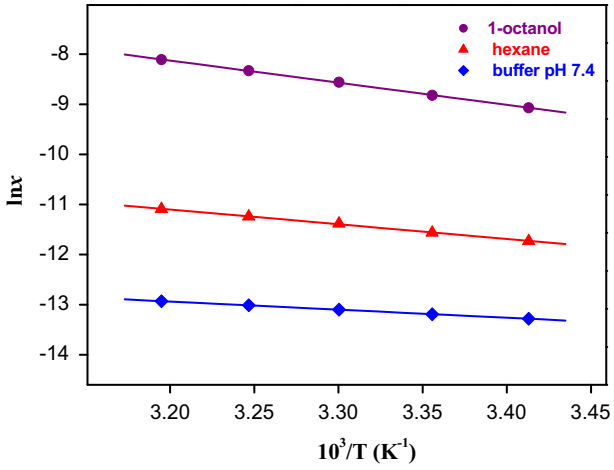

Fig. 3. Temperature dependencies of solubility of the compound I in selected solvents.

Table 3
Experimental mole fraction solubilities (x) of the compounds studied in buffer pH 7.4, hexane and 1-octanol at different temperatures.

T (K)	I			II			III		
	Buffer pH 7.4	Hexane	1-octanol	Buffer pH 7.4	Hexane	1-octanol	Buffer pH 7.4	Hexane	1-octanol
	$x \cdot 10^6$	$x \cdot 10^6$	$x \cdot 10^4$	$x \cdot 10^6$	$x \cdot 10^5$	$x \cdot 10^4$	$x \cdot 10^6$	$x \cdot 10^5$	$x \cdot 10^4$
293.15	1.69	7.96	2.16	1.64	1.42	0.89	5.57	3.30	0.71
298.15	1.86	9.41	2.74	1.96	1.70	1.13	6.55	3.71	0.93
303.15	2.04	11.41	3.48	2.27	2.02	1.39	7.53	4.18	1.22
308.15	2.23	13.26	4.28	2.70	2.35	1.68	8.77	4.68	1.61
313.15	2.42	15.50	5.40	3.21	2.72	2.11	10.09	5.31	2.05
A[a]	−7.76 ± 0.04	−1.25 ± 0.18	5.83 ± 0.11	−2.90 ± 0.22	−1.39 ± 0.17	3.95 ± 0.23	−2.82 ± 0.09	−2.93 ± 0.14	7.10 ± 0.15
B[a]	1649 ± 12	3073 ± 39	4179 ± 45	3054 ± 67	2989 ± 49	3889 ± 69	2719 ± 29	2165 ± 43	4876 ± 47
R[b]	0.9999	0.9997	0.9998	0.9993	0.9996	0.9995	0.9998	0.9994	0.9999
σ[c]	$0.2 \cdot 10^{-2}$	$0.9 \cdot 10^{-2}$	$0.8 \cdot 10^{-2}$	$1.1 \cdot 10^{-2}$	$0.8 \cdot 10^{-2}$	$1.2 \cdot 10^{-2}$	$0.4 \cdot 10^{-2}$	$0.7 \cdot 10^{-2}$	$1.2 \cdot 10^{-2}$

T (K)	IV			V		
	Buffer pH 7.4	Hexane	1-octanol	Buffer pH 7.4	Hexane	1-octanol
	$x \cdot 10^6$	$x \cdot 10^4$	$x \cdot 10^4$	$x \cdot 10^6$	$x \cdot 10^4$	$x \cdot 10^4$
293.15	8.34	3.85	2.51	2.66	5.42	1.15
298.15	9.60	4.47	3.01	3.25	6.39	1.47
303.15	11.11	5.11	3.68	4.01	7.47	1.91
308.15	12.66	5.96	4.39	4.95	8.87	2.42
313.15	14.60	6.81	5.30	6.07	10.22	3.01
A[a]	−2.96 ± 0.09	1.09 ± 0.1	3.65 ± 0.15	0.12 ± 0.16	2.45 ± 0.12	6.03 ± 0.15
B[a]	2558 ± 27	2624 ± 30	3501 ± 46	3799 ± 50	2922 ± 38	4423 ± 47
R[b]	0.9998	0.9998	0.9997	0.9998	0.9997	0.9998
σ[c]	$0.4 \cdot 10^{-2}$	$0.5 \cdot 10^{-2}$	$1.0 \cdot 10^{-2}$	$0.84 \cdot 10^{-2}$	$0.7 \cdot 0^{-2}$	$0.8 \cdot 10^{-2}$

[a] Parameters of the correlation equation: $\ln x = A - B/T$.
[b] R – pair correlation coefficient.
[c] σ – standard deviation.

group). The dissociation constant values (Table 2) indicate that all the studied substances have almost the same protolytic properties and are strong acids, which is explained by the presence of an NH-group in the triazol-thion heterocycle. The content of ionized and nonionized molecule forms depending on the pH of the water solution was determined based on pK_a values using the Henderson-Hasselbach equation (Po and Senozan, 2001). As Fig. 4 shows, the molecules of the studied compounds are in the neutral state at pH < 7.0, while at pH > 7.0 they act as acids and become deprotonated. In the buffer solution (pH 7.4) all the molecules are in the neutral form.

All the studied compounds have very low solubility in the buffer (pH 7.4), with the solubility values ranging between $(1.86–46.2) \cdot 10^{-6}$ mole fractions at the temperature of 298.15 K. As it has determined, the solubility values of the substances can be arranged as follows: **I** < **II** < **V** < **III** < **IV** (Fig. 5). Substitution of the hydrogen atom in the benzene ring of compound **I** for a methyl group and transformation of the latter into compound II slightly increase the solubility in the aqueous medium. In this case, the influence of the methyl group on the solubility of the mentioned heterocyclic compound results from this substituent ability to disrupt the formation of hydrogen-bonded water associates and is not the direct effect of the electron density shift (Albert, 2007). Compounds **III**–**V** with halogen atoms and a methoxy-group as substituents have a comparatively higher solubility in the buffer.

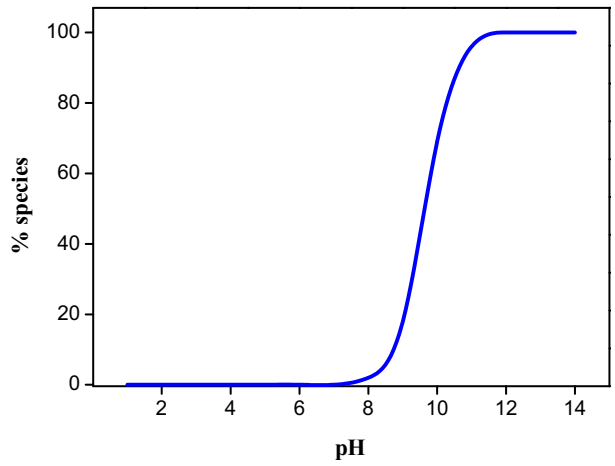

Fig. 4. Distribution of species as function of pH of buffer solution for compounds **I**–**V**.

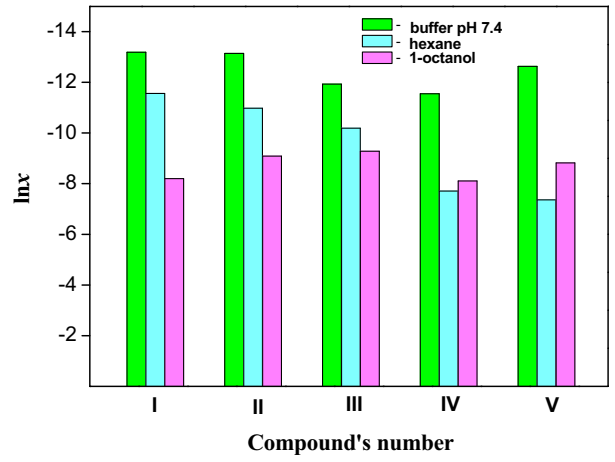

Fig. 5. Solubility histogram of compounds studied.

The polar groups in these compounds probably produce an inductive effect shifting the electrons of the benzene ring to the atoms of fluorine, chlorine and oxygen, which results in stronger dipole-dipole interactions of the dissolved substances with the water molecules and higher solubility. And the best solubility is observed in compound **IV** with a fluorine atom that is the most electronegative element.

The solubility of the studied compounds in hexane is almost an order of magnitude higher than in the buffer solution but does not exceed the value of $4.87 \cdot 10^{-4}$ mole fractions at the standard temperature. The only exception is unsubstituted derivative **I**, the solubility of which increases by 5 times only. Since hexane can interact with substances only through van-der-Waals forces, introduction of substituents is characterized by higher solubility of the compounds due to induced dipoles formed in the molecule aromatic ring and the resulting attraction between the dissolved substance and the solvent. The electron donating methyl group of compound **II** increases the electron density of the aromatic ring and, consequently, the strength of interaction with hexane, which improves the solubility. The inductive effect of the oxygen atoms and halogens results in electron shift toward electron accepting substituents. And it is quite natural that substitution of the C—H bond for C—OCH_3, C—Cl and C—F bonds increases the solubility of the compounds as the atoms become more electronegative. Besides, it has been found that the solubility of derivatives **II**–**V** in hexane increases in the same order as their melting temperatures decrease (Table 2).

The data in Table 3 show that the substances solubility in 1-octanol is also very low, with the values between $(0.71–5.40) \cdot 10^{-4}$ mole fractions in the studied temperature range. In the order of increasing solubility in this solvent the compounds are arranged as follows: **III** < **II** < **V** < **I** < **IV**. And the values of solubility are higher in 1-octanol than in the aqueous solution for all the compounds. Introduction of methyl- and methoxy-substitutents into the benzene ring insignificantly increases the solubility of compounds **II** and **III** in alcohol compared to hexane. The opposite effect is observed when the oxygen atoms are replaced with halogen ones in the benzene ring: the solubility values of compounds **IV** and **V** in 1-octanol are lower than in hexane. Therefore, despite the presence of an active hydroxy-group in the molecules of 1-octanol and electronegative chlorine and fluorine atoms in the structure of the dissolved substances, the solubility is not determined by the hydrogen bonding ability but by non-specific salvation. It is worth noting that the low solubility of the studied substances in 1-octanol is also caused by stronger association and bigger molar volume of alcohol molecules compared to those of hexane, which hinders the penetration of the molecules of the dissolved substance into the free cavity of the solvent.

The solubility data are represented as linear functions ln*x versus* 1/T, and the thermodynamic solubility parameters of the compounds in buffer (pH 7.4), hexane and 1-octanol are calculated by Eqs. (2)–(5) and summarized in Table 4. In all the studied systems "dissolved substance – solvent", the solubility enthalpies are positive, which indicates the endothermicity of the solubility processes. The systems with hexane have the lowest solution enthalpy values for the studied substances. These values are higher in water solutions and the highest in the systems with 1-octanol. The negative entropy contribution makes the Gibbs energy higher and, as a result, lowers the substance solubility in the buffer and hexane. On the opposite, the positive entropy values characterizing the dissolution process of compounds **IV** and **V** in hexane increase the solubility of these substances up to the values exceeding their solubility in 1-octanol. When these compounds are dissolved in 1-octanol, their high positive enthalpy and entropy contributions

Table 4
Thermodynamic solubility functions of compounds studied in buffer pH 7.4, hexane and 1-octanol at 298.15 K.

Com-pound	[a]ΔG^0_{sol} (kJ/mol)	[b]ΔH^0_{sol} (kJ/mol)	[c]ΔS^0_{sol} (J/mol·K)	ΔG^0_{sol} (kJ/mol)	ΔH^0_{sol} (kJ/mol)	ΔS^0_{sol} (J/mol·K)	ΔG^0_{sol} (kJ/mol)	ΔH^0_{sol} (kJ/mol)	ΔS^0_{sol} (J/mol·K)
	Buffer pH 7.4			Hexane			1-octanol		
I	32.7	13.7	-63.73	28.6	25.6	-6.7	20.3	34.7	69.9
II	32.6	25.4	-24.2	27.2	24.9	-7.7	22.5	32.3	32.9
III	29.6	22.6	–23.4	25.3	18.0	-24.5	23.0	40.5	58.7
IV	28.6	21.3	-24.6	19.1	21.8	9.1	20.1	29.1	30.2
V	30.7	31.6	2.9	18.2	24.3	13.1	21.9	36.8	50.0

[a] ΔG^0_{sol} – standard molar dissolution Gibbs energy.
[b] ΔH^0_{sol} – standard molar dissolution enthalpy.
[c] ΔS^0_{sol} – standard molar dissolution entropy.

produce a compensation effect on the Gibbs energy. As a result, the solubility of compounds **I**–**III** in 1-octanol is higher, while that of compounds **IV** and **V** is lower than in hexane.

Based on the obtained data about the solubility and ability of the synthesized substances to block glutamate-induced calcium ion uptake into synaptosomes of rat cerebral cortex, the comparison their biological activity at the concentration of 1 μM corresponding to the maximum Dimebon activity in this test was carried out. The analysis has shown that the best inhibition parameters (~17%) are characteristic of derivatives **III** with a methoxy-group and **IV** with a fluorine atom as the substituent. These compounds are better soluble in the buffer (pH 7.4) and compound **IV** also dissolves in hexane and 1-octanol better than the other derivatives.

4. Conclusion

In this study, hydrogenated pyrido[4,3-b]indoles as potential drug compounds with neurocorrecting activity have been synthesized. The obtained compounds differ in the chemical nature of the substituent (H—, CH_3—, CH_3O—, F— Cl—) introduced into position 8 of the carboline fragment of the molecule. The biological tests have shown that all the studied compounds can modulate glutamate-dependent uptake of calcium ions in rat cerebral cortex synaptosomes. The compound with a methoxy-substituent has been found to have the highest inhibiting activity within a broad concentration range, which allows to recommend it as the object of further research.

The shake-flask method was used to measure the solubility of the studied compounds in pharmaceutically relevant media: buffer solution (pH 7.4), hexane and 1-octanol. It was identified that all the derivatives in these solvents have a very low solubility not exceeding the value of 8 10^{-4} mole fractions. And the compounds with a methoxy-group and a fluorine atom as substituents are best soluble in the buffer solution (pH 7.4) modeling the blood plasma medium.

In order to find the reasons for the poor solubility of the studied compounds, their thermophysical and protolytic properties were analyzed. By using the DCS method it have found that these substances melt at the temperature above 230 °C. This indirectly proves that the crystal lattice energy of the compounds is high and is one of the factors lowering the solubility. Besides, the obtained experimental and calculation data have shown that in the studied solutions the molecules are in neutral form and interact with the solvent only through non-specific salvation, which also increases the solubility. Based on the temperature dependences of solubility, the thermodynamic functions of substance dissolution in the solvents used have been calculated. In the studied systems "dissolved substance – solvent", the dissolution processes are endothermic. In all the studied substances, when the substituent is replaced, the solution enthalpy increases in the following order: hexane, buffer (pH 7.4), 1-octanol.

Acknowledgments

This work was supported by the grant of RFBR No. 18-43-370016 r_a.

References

Albert, A., 2007. Selective Toxicity: The Physico-Chemical Basis of Therapy. Chapman and Hall, London.
Archer, D.G., Steffen, P., Rudtsch, J., 2003. Enthalpy of fusion of indium: a certified reference material for differential scanning calorimetry. J. Chem. Eng. Data 48, 1157–1163. https://doi.org/10.1021/je030112g.
Asirvatham, S., Dhokchawle, B.V., Tauro, S.J., 2016. Quantitative structure activity relationships studies of non-steroidal anti-inflammatory drugs: a review. J. Chem. Arab. https://doi.org/10.1016/j.arabjc.2016.03.002.
Avdeef, A., 2007. Solubility of sparingly-soluble ionizable drugs. Adv. Drug Deliv. Rev. 59, 568–590. https://doi.org/10.1016/j.addr.2007.05.008.
Baka, E., Comer, J.E.A., Takacs-Novak, E., 2008. Study of equilibrium solubility measurement by saturation shake-flask method using hydrochlorothiazide as model compound. J. Pharm. Biomed. Anal. 46, 335–341. https://doi.org/10.1016/j.jpba.2007.10.030.
Blokhina, S.V., Volkova, T.V., Ol'khovich, M.V., Sharapova, A.V., Proshin, A.N., Bachurin, S.O., Perlovich, G.L., 2014. Synthesis, biological activity, distribution and membrane permeability of novel spirothiazines as potent neuroprotectors. Eur. J. Med. Chem. 77, 8–17. https://doi.org/10.1016/j.ejmech.2014.02.052.
Dondas, H.A., Hempshall, A., Narramore, S., Kilner, C., Fishwick, C.W.G., Grigg, R., 2016. γ-Carboline AC190 analogues via palladium catalysed allene insertion stereo and regioselective 3- and 5-component cascades. Tetrahedron 72, 1316–1329. https://doi.org/10.1016/j.tet.2016.01.025.
Doody, R.S., Gavrilova, S.I., Sano, M., Thomas, R.G., Aisen, P.S., Bachurin, S.O., Seely, L., Hung, D., 2008. Effect of dimebon on cognition, activities of daily living, behaviour, and global function in patients with mild-to-moderate Alzheimer's disease: a randomised, double-blind, placebo-controlled study. Lancet 372, 207–215. https://doi.org/10.1016/S0140-6736(08)61074-0.
Du-Cuny, L., Huwyler, J., Wiese, M., Kansy, M., 2008. Computational aqueous solubility prediction for drug-like compounds in congeneric series. Eur. J. Med. Chem. 43, 501–512. https://doi.org/10.1016/j.ejmech.2007.04.009.
Eckert, G.P., Renner, K., Eckert, S.H., Eckmann, J., Hagl, S., Abdel-Kader, R.M., Kurz, C., Leuner, K., Muller, W.E., 2012. Mitochondrial dysfunction – a pharmacological target in Alzheimer's disease. Mol. Neurobiol. 46, 136–150. https://doi.org/10.1007/s12035-012-8271-z.
Faller, B., Erlt, P., 2007. Computational approaches to determine drug solubility. Adv. Drug Deliv. Rev. 59, 533–545. https://doi.org/10.1016/j.addr.2007.05.005.
Farlow, M.R., 2004. NMDA receptor antagonists: a new therapeutic approach for Alzheimer's disease. Geriatrics 59, 22–27.
Gylys, K.H., Fein, J.A., Cole, G.M., 2000. Quantitative characterization of crude synaptosomal fraction (P-2) components by flow cytometry. J. Neurosci. Res. 15, 186–192. https://doi.org/10.1002/1097-4547(20000715)61:2<186::AID-JNR9>3.0.CO;2-X.
Hajos, F., 1975. An improved method for the preparation of synaptosomal fractions in high purity. Brain Res. 93, 485–489. https://doi.org/10.1016/0006-8993(75)90186-9.
Hung, D.T., Protter, A.A., Jain, R.P., Dugar, S., Chakravarty, S., 2015. Tetracyclic compounds. Patent US8999978 B2.
Ikonomidou, C., Turski, L., 2002. Why did NMDA receptor antagonists fail clinical trials for stroke and traumatic brain injury? Lancet Neurol. 1, 383–386. https://doi.org/10.1016/S1474-4422(02)00164-3.
Ivachtchenko, A.V., Frolov, E.B., Mitkin, O.D., Tkachenko, S.E., Khvat, A.V., 2010. Synthesis and biological activity of 5-styryl and 5-phenethyl-substituted

2,3,4,5-tetrahydro-1H- pyrido[4,3-b]indoles. Bioorg. Med. Chem. Let. 20, 78–82. https://doi.org/10.1007/s10593-010-0488-z.
Khachaturian, Z.S., 1994. Calcium hypothesis of Alzheimer's disease and brain aging. Ann. N. Y. Acad. Sci. 747, 1–11. https://doi.org/10.1111/j.1749-6632.1994.tb44398.x.
Khan, A.U., 2016. Descriptors and their selection methods in QSAR analysis: paradigm for drug design. Drug Discov. 21, 1291–1302. https://doi.org/10.1016/j.drudis.2016.06.013.
Kerns, E., Di, L., 2008. Drug like Properties: Concepts, Structure Design and Methods. Academic Press, New York.
Mattson, M.P., Cheng, B., Davis, D., Bryant, K., Lieberburg, I., Rydel, R.E., 1992. β-Amyloid peptides destabilize calcium homeostasis and render human cortical neurons vulnerable to excitotoxicity. J. Neurosci. 12, 376–389.
Parsons, C.G., Danysz, W., Quack, G., 1998. Glutamate in CNS disorders as a target for drug development: an update. Drug News Perspect. 11, 523–579.
Perlovich, G.L., Volkova, T.V., Bauer-Brandl, A., 2006. Towards an understanding of the molecular mechanism of solvation of drug molecules: a thermodynamic approach by crystal lattice energy, sublimation, and solubility exemplified by paracetamol, acetanilide, and phenacetin. J. Pharm. Sci. 95, 2158–2169. https://doi.org/10.1002/jps.20674.
Po, H.N., Senozan, N.M., 2001. Henderson-Hasselbalch equation: its history and limitations. J. Chem. Educ. 78, 1499–1503. https://doi.org/10.1021/ed078p1499.
Rekker, F.R., Mannhold, R., 1992. Calculation of Drug Lipophilicity: The Hydrophobic Fragmental Constant Approach. VCH, Weinheim.
Sharapova, A., Ol'khovich, M., Blokhina, S., Perlovich, G., 2017. Physico-chemical characterization antituberculosis thioacetazone: vapor pressure, solubility and lipophilicity. J. Chem. Thermodyn. 108, 18–25. https://doi.org/10.1016/j.jct.2017.08.012.
Steele, J.W., Gandy, S., 2013. Latrepirdine (Dimebon®), a potential Alzheimer therapeutic, regulates autophagy and neuropathology in an Alzheimer mouse model. Autophagy 9, 617–618. https://doi.org/10.4161/auto.23487.
Stefek, M., Tsantili-Kakoulidou, A., Milackova, I., Juskova, M., Triantos, N., 2011. (2-Benzyl-2,3,4,5-tetrahydro-1H-pyrido[4,3-b]indol-8-yl)-acetic acid: An aldose reductase inhibitor and antioxidant of zwitterionic nature. Bioorg. Med. Chem. 19, 7181–7185. https://doi.org/10.18388/abp.2014_953.
Stephen, H., Stephen, T., 1963. Solubilities of Inorganic and Organic Compounds. Oxford Pergamon, London.
Van de Waterbeemd, H., Rose, S. 2008. Quantitative approaches to structure – activity relationships, third ed. In: Wermuth, C., (Ed.), The Practice of Medicinal Chemistry, pp. 491–513.